

# Plasmonic sub-wavelength phase-gradient meta-surfaces for real time dispersive imaging

Yuewang Huang, Qiancheng Zhao, Salih K. Kalyoncu, Rasul Torun, Yumeng Lu, Filippo Capolino & Ozdal Boyraz

EECS Department, University of California, Irvine, CA 92697

Author e-mail address: [oboyraz@uci.edu](mailto:oboyraz@uci.edu)

**Abstract:** We have designed and fabricated a sub-wavelength plasmonic deflector based on phase-gradient meta-surfaces for dispersion imaging at 1.55 $\mu\text{m}$ . We demonstrate dispersive imaging with <300 $\mu\text{m}$  resolution and 75.6% power efficiency by incorporating the fabricated plasmonic deflectors.

To achieve light manipulation in micro/nano-scale, sub-wavelength scale wavefront manipulation is necessary. Among the many methods proposed for wavefront engineering, the metal-insulator-metal (MIM) structure as in inset of Fig.1, known as MIM meta-surface, has the advantage of high efficiency and conservation of polarization compared to meta-material and single layer meta-surface [1-4]. Here, we designed and fabricated a phase-gradient deflector based on MIM meta-surface consist of a metallic patch array for imaging applications at 1550nm, which is similar to the MIM structure studied in [3,4]. Linear phase gradient is achieved by tuning the size of the metal patches on the top and hence normal incident light is deflected to an angle determined by the phase-gradient. The fabricated sub-wavelength meta-surface plasmonic deflector (MSPD) device operated in the near infrared telecommunication window. For the center wavelength of 1.55 $\mu\text{m}$ , normally incident TE polarized light was deflected to an angle of  $\sim 51^\circ$  with a high power efficiency of 75.6%. The deflector showed an angular dispersion of  $\sim 0.4^\circ/10\text{nm}$ . We also integrated the MSPD into a dispersive Fourier transform imaging system and experimentally demonstrated an imaging resolution of <300 $\mu\text{m}$ .

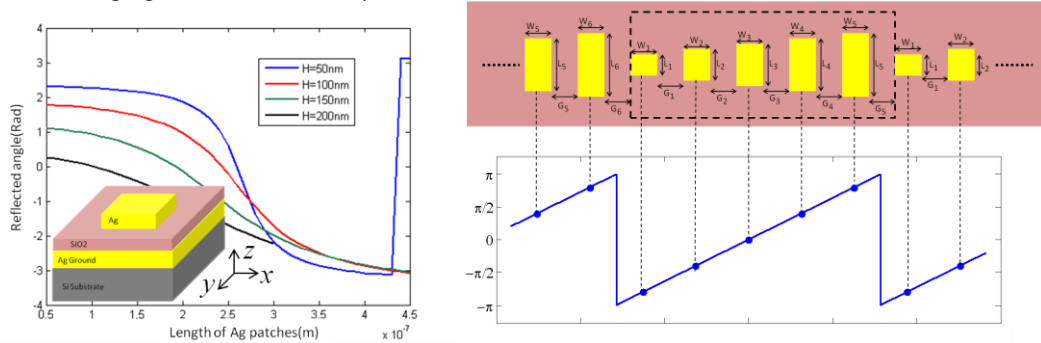


Fig. 1. (a) Phase of reflectivity for MIM plasmonic structure with different geometrical parameters. (Inset) A unit cell of the designed MIM structure. (b) Schematics showing the design principle of the sub-wavelength meta-surface plasmonic deflector (MSPD). Dash line enclosed a super-cell.

The inset of Fig.1 (a) shows the stack of the designed MIM unit cell. Silver (Ag) and silicon dioxide ( $\text{SiO}_2$ ) are used as the metal and dielectric due to their superior loss property at near-IR wavelength. Proper combination of the geometry parameters in the unit cell can excite plasmonic resonance in MIM structure. In the vicinity of resonance, the phase of the complex reflectivity function is sensitive to the size of the metallic patches as shown in Fig. 1(a). When the oxide thickness is 50nm, the phase of the reflectivity can be tuned for a range of nearly  $2\pi$ , which can theoretically generated any phase profile. To generate a linear phase-gradient, 5 sub-cells with different Ag patch lengths are combined to form a super-cell spanning over a phase variation of  $2\pi$  in a linear fashion. According to the phase plots in Fig. 1(a), we determine the patch lengths as  $L_1=171\text{nm}$ ,  $L_2=236\text{nm}$ ,  $L_3=254\text{nm}$ ,  $L_4=273\text{nm}$  and  $L_5=350\text{nm}$ . The structure repeats itself for every period  $\Lambda=2\mu\text{m}$  and this gives a phase gradient of  $(\nabla\mathbf{k})_x = 2\pi/\Lambda$  along X direction. For the designed wavelength of 1.55 $\mu\text{m}$  at normal incidence, this equals to the X component of the wave vector of deflected wave and implies a reflected angle of  $\sin^{-1}\{(\nabla\mathbf{k})_x/k_0\} = 50.8^\circ$  theoretically.

To fabricate the device, we started with a prime silicon substrate. Ground plane Ag and oxide spacer was first deposited using E-beam evaporation. Double layer PMMA and E-beam lithography was used to pattern the complimentary structure of the top layer. After evaporation of the top Ag layer, lift-off in acetone was employed to finally define the top Ag pattern. A SEM image of the fabricated MSPD device is shown in Fig. 3(a). We also tested the fabricated device using a tunable laser. Fig. 3(b) shows the measured deflected angle with respect to wavelength along with simulated deflected angles. Due to limitation on angular resolution and wavelength tuning range, only

five different wavelengths were measured. Fig. 3(c) shows the deflected angle for different incident angle at the wavelength of 1.55 $\mu\text{m}$ . Deflected angle is quite different from the incident angle, clearly revealing the phenomena of anomalous reflection [1]. Due to experimental setup limitation, we only have measurement result for incident angle up to  $\sim 8^\circ$ . As incident angle increases, the power efficiency drops. Simulation shows that there is no deflection when the incident angle is greater than  $12^\circ$ . This can be explained as follows. With both oblique incidence and surface phase gradient present, the wave propagation constant along X direction will be  $(\nabla\mathbf{k})_x = \frac{2\pi}{\Lambda} + \mathbf{k}_0 \sin \theta_i$ . When  $(\nabla\mathbf{k})_x > \mathbf{k}_0$ , no reflection will be supported. For a wavelength of 1.55 $\mu\text{m}$ , this gives a critical angle of  $\theta_c = 13^\circ$ . In fact, the incident wave can couple to the surface plasmonic wave after the critical angle [3]. The measured and simulated results show very good agreement and we accounted the slight smaller angle in the measurement to be systematic error in experiment setup and/or fabrication, inaccurate electromagnetic constants of materials in simulation, and the aging of top Ag layer. The measured power efficiency for TE-polarized light at 1.55 $\mu\text{m}$  is  $\sim 75.6\%$ . This also agrees well with the simulated efficiency of 81.3%.

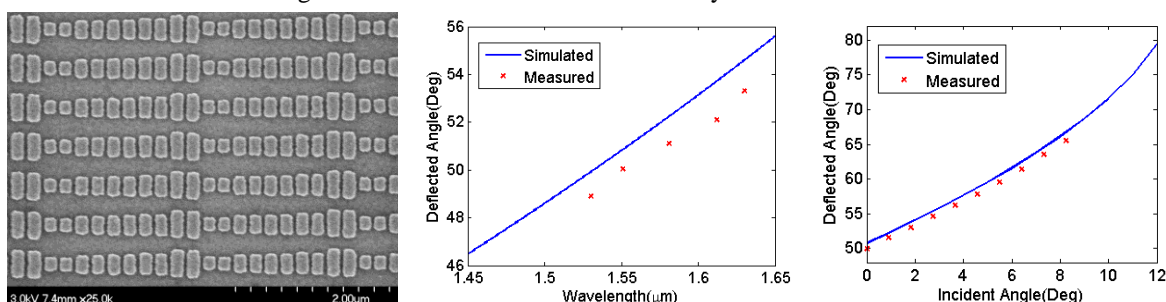


Fig. 2 (a) The SEM image of the fabricated device; (b) simulated and measured deflected angle for different wavelengths with normal incidence. (c) simulated and measured deflected angle for different incident angle at 1.55 $\mu\text{m}$ .

After verification of the functionality of the MSPD device, we inserted it into the dispersive image system to replace conventional grating as shown in Fig. 4(a) [5,6]. Supercontinuum laser pulse with wavelength from 1580nm to 1600nm passes through the fiber-based dispersion unit with 675ps/nm. This dispersive Fourier Transform process expands the pulse to 13ns and map different wavelength to different time (short wavelength to leading edge and long wavelength to trailing edge). We then turn on the DMD's row by row from top to bottom to achieve scanning in the vertical direction. With the current state of art mirror technology, up to 32.5kHz flip speed can be readily achieved. This means we can scan at a speed of 30 $\mu\text{s}$ /row. As an example, Fig. 4(b) shows the recovered image of Element 4 in Group 0 of 1951 USAF. The vertical lines width and spacing are 354.6 $\mu\text{m}$ . We can resolve lines  $< 300\mu\text{m}$  using this imaging system. This demonstrated a solid application of the designed MSPD device. We can further increase the resolution capability by using a MSPD device with large fingerprint.

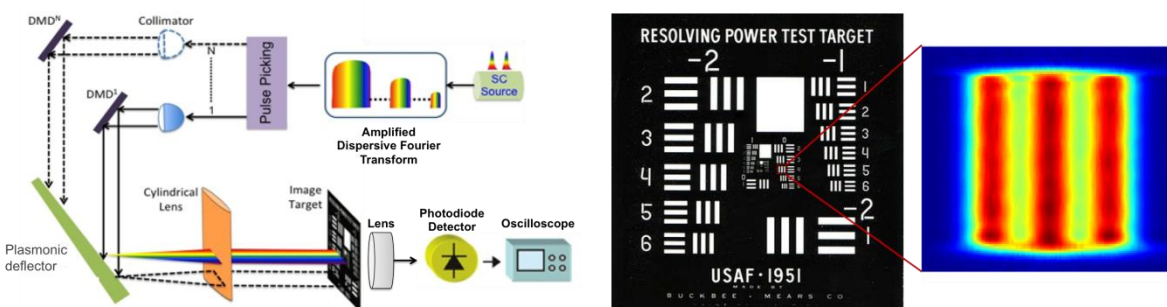


Fig. 3 (a) The setup of the imaging system using the fabricated deflective device; (b) Imaged pattern on USAF test chart Element 4 in Group 0 with line-width of 354.6 $\mu\text{m}$ . A resolution  $< 300\text{nm}$  can be achieved.

This research is supported by National Science Foundation (NSF) Award # ECCS-1028727.

- [1] Yu, N., Genevet, P., Kats, M. A., Aieta, F., Tetienne, J. P., Capasso, F., & Gaburro, Z. *Science*, 334(6054), 333(2011)
- [2] Yu, N.; Genevet, P.; Aieta, F.; Kats, M.A.; Blanchard, R.; Aoust, G.; Tetienne, J.-P.; Gaburro, Z.; Capasso, F., *IEEE Sel. Top. Quant. Electron.* 19(3), 4700423(2013)
- [3] S. Sun, Q. He, S. Xiao, Q. Xu, X. Li, and L. Zhou, *Nat. Mater.* 11, 426–431 (2012).
- [4] S. Sun, K.-Y. Yang, C.-M. Wang, T.-K. Juan, W. T. Chen, C. Y. Liao, Q. He, S. Xiao, W.-T. Kung, G.-Y. Guo, L. Zhou, and D. P. Tsai, *Nano Lett.* 12, 6223–6229 (2012).
- [5] Kalyoncu, S.K.; Yuewang Huang; Qi Song; Boyraz, O., *Photonics Journal, IEEE* 5(1), 5500207(2013).
- [6] S. K. Kalyoncu, Y. Huang, R. Torun, Q. Zhao, and O. Boyraz, *CLEO: 2013*, paper JT4A.30.